Electronic Supplementary Information

Preclinical Evaluation of Platinum-Loaded Hydroxyapatite Nanoparticles in an embryonic zebrafish xenograft model

Robin A. Nadar[a,‡], Nandini Asokan[b,c,‡], Lorenzo Degli Esposti[d], Alessandra Curci[e], Alessandra Barbanente[e], Lukas Schlatt[f], Uwe Karst[f], Michele Iafisco[d], Nicola Margiotta[e], Michael Brand[b], Jeroen J. J. P. van den Beucken[a], Martin Bornhäuser[b,c,g,h] and Sander C. G. Leeuwenburgh[a,d,*]

[a]Department of Dentistry - Regenerative Biomaterials, Radboud Institute for Molecular Life Sciences, Radboud University Medical Center, Philips van Leydenlaan 25, 6525 EX Nijmegen, the Netherlands.
[b]Center for Regenerative Therapies Dresden (CRTD), Technische Universität Dresden, Fetscherstrasse 105, 01307 Dresden, Germany.
[c]Division of Hematology, Oncology and Stem Cell Transplantation, Department of Medicine I, University Hospital Carl Gustav Carus, Technische Universität Dresden, Fetscherstrasse 74, 01307 Dresden, Germany.
[d]Institute of Science and Technology for Ceramics (ISTEC), National Research Council (CNR), Via Granarolo 64, 48018 Faenza, Italy.
[e]Dipartimento di Chimica, Università degli Studi di Bari Aldo Moro, Via E. Orabona 4, 70125 Bari, Italy.
[f]Institute of Inorganic and Analytical Chemistry, University of Münster, Corrensstraße 30, 48149 Münster, Germany.
[g]National Center for Tumor Diseases (NCT), Fetscherstrasse 74/PF 64, 01307 Dresden, Germany.
[h]German Consortium for Translational Cancer Research (DKTK), DKFZ, D-69120 Heidelberg, Germany.

‡Authors contributed equally

† Electronic supplementary information (ESI) available

*Corresponding author
Email: sander.leeuwenburgh@radboudumc.nl

Experimental Section

Instrumentation

^{1}H-NMR, ^{31}P-NMR and ^{195}Pt-NMR spectra were recorded on Bruker Avance DPX 300 MHz, Bruker Avance II 600 MHz and Bruker Avance III 700 MHz instruments at the Department of Chemistry of the University of Bari Aldo Moro (Bari, Italy). Standard pulse sequences were used for ^{1}H, $^{31}P\{^{1}H\}$(121.5 and 242.9 MHz, respectively), and $^{195}Pt\{^{1}H\}$ (64.5 MHz) 1D spectra. ^{1}H chemical shifts were referenced using the internal residual peak of the solvent (D_2O: 4.80 ppm). ^{31}P chemical shifts were referenced to external H_3PO_4 (85% w/w). ^{195}Pt chemical shifts were referenced to external $K_2[PtCl_4]$ in D_2O fixed at −1628 ppm. Electrospray ionization mass spectrometry (ESI-MS) was performed with a dual electrospray interface and a quadrupole time-of-flight mass spectrometer (Agilent 6530 Series Accurate-Mass Quadrupole Time-of-Flight (Q-TOF) LC-MS). Elemental analyses were carried out with a Eurovector EA 3000 CHN instrument. The H138 miniLab, a portable pH meter with an ISFET pH sensor were used for pH measurements.

Characterization of hydroxyapatite nanoparticles

The lyophilized hydroxyapatite powders were characterized by FT-IR and powder X-ray Diffraction (XRD). The infrared spectra were recorded in the wavelength range from 4000 to 400 cm^{-1} with 1 cm^{-1} resolution using an attenuated total reflectance Fourier transform infrared spectrometer (ATR-FTIR Spectrum One, Perkin Elmer). The X-ray diffraction (XRD) patterns of the powders were recorded with a PANalytical X'Pert^3 Powder equipped with a Xenon point detector using Cu Kα radiation (λ = 1.5405 Å) generated at 40kV and 40 mA. The instrument was configured with receiving and divergence slits of 1/16° and 1°, respectively. The 2θ range was from 5° to 60° with a step size (2θ) of 0.02° and a counting time of 2 sec. The crystal domain sizes, along the HA axis directions, were calculated using Scherrer's equation (1):

$$L_{(0,0,2)} = \frac{0{,}94\lambda}{\left[\cos\theta\left(\sqrt{\Delta_r^2 - \Delta_0^2}\right)\right]} \quad (1)$$

where θ is the diffraction angle for plane (002), Δ*r* and Δ_0 the full widths at half maximum (FWHM) in radians of reflection (002) for the synthesized HA materials, respectively, and *λ* = 1.5405 Å. Further, the morphology and size of the nanoparticles were confirmed by Transmission Electron Microscopy (TEM, JEOL 1010). The samples were dispersed in ethanol at the concentration of 0.5 mg/mL and then 2 µl of solution were deposited on copper grids. The size of HA NPs was determined by averaging the length of at least 50 particles using TEM images by digital image analysis software (Image J, NIH).

DLS analysis

The nanoparticles suspension after purification were diluted 1:10 in water (about 0.5 mg/mL) and were analyzed by Dynamic Light Scattering (DLS) and laser doppler electrophoresis in order to determine the hydrodynamic diameter, polydispersity index

(PdI) and the surface zeta potential. The nanoparticle suspensions were characterized by DLS using a Zetasizer Nano Series (Malvern, UK) by backscatter detection (λ = 630 nm, θ = 173°). Particle size (reported as Z-average of hydrodynamic diameter) was calculated as the average of three measurements of 10 runs for 10 s at 25 °C. Zeta potential measurements through electrophoretic mobility were carried out with a Zetasizer Nano analyzer (Malvern, UK) using disposable folded capillary cells (DTS1061; Malvern, UK) at 25 °C. Three separate measurements (100 runs each) were collected in each case.

Dye labeling of HA nanoparticles

To determine the minimum concentration of AF647-zoledronate required for satisfactory labeling of HA nanoparticles, 1 or 2 nmol AF647-zoledronate were dissolved in 100 µL of MilliQ and mixed with 10 mg of HA (900 µL of suspension). The suspension was kept under agitation at 37 °C for 2 h, and subsequently washed twice by centrifugation (2500 x g, 5 minutes). Further, labeling was confirmed by spectrophotometric analysis of the supernatant using UV-VIS spectroscopy at a wavelength of 648 nm. The labeled nanoparticles were further investigated using DLS to confirm the size, dispersion and change in zeta potential.

***In vivo* studies**

Ototoxicity assay

The lateral line neuromast hair cells in *casper* embryos were stained with a vital dye to analyse the loss of hair cells due to the treatment with PtPP. Cisplatin was used as positive control, since this compound effectively reduces hair cell viability in zebrafish. The fluorescent dye 2-[4-(dimethylamino) styryl]-N-ethylpyridinium iodide (DASPEI)

[Molecular Probes, Eugene, OR] was used to stain hair cells within neuromasts, as described previously.[1] Zebrafish embryos were incubated in embryo medium containing 0.005 % DASPEI for 15 min, anesthetized in Tricaine MS222 (10 µg/ml) for 5 min, rinsed once in fresh embryo medium, and imaged using confocal microscope (Zeiss LSM 780). The quantification of the number of neuromast hair cells from one side of the embryo was done manually under the microscope.

Neurotoxicity assay

Cell death in the brains of PtPP-treated zebrafish larvae and untreated controls was analysed using the TUNEL assay combined with HuC/D staining. 4 dpf embryo, at 2 days post treatment, were terminally anaesthetized with MESAB, fixed in 2 % PFA / 1 % DMSO for at least overnight at 4 ºC and stored until use. To harvest the brains, larvae was washed with PBS and dissected under a stereo microscope. The collected brain samples were depigmented with bleaching solution. The TUNEL assay was performed using the ApopTag Red/Fluorescein In Situ Apoptosis Detection Kit. For larva brains alone, the manufacturer's instructions were adjusted as follows. Cleared larvae brains were washed with Sodium Citrate/ 0.1 % PBSTx (Phosphate-buffered saline with Triton X-100), 3 times 10 min at room temperature, post-fixed with -20 ºC-cold Acetone/Ethanol (2:1) for 15 min at -20 ºC washed with PBSTx 3 times for 5 min, and incubated in Equilibration Buffer for 1 h at room temperature. TdT (Terminal deoxynucleotidyl transferase) Enzyme, Stop/Wash solutions and the anti-DIG antibody were used according to recommendations. After the TUNEL assay, brains were stained for HuC/D using an antibody staining protocol described earlier that included a prior antigen retrieval step for HuC/D as follows. Brains were incubated in 98 ºC Tris-HCl buffer (pH 8.0) for 5 min at 98 ºC, washed with PBSTx (3times* 5 min) at room

temperature. Confocal images of stained brains were acquired on a Zeiss LSM 780 upright confocal microscope using C-Apochromat 10X/0.45 W and LD LCI Plan-Apochromat 25X/0.8 Imm Corr DIC M27 objectives for water immersion.

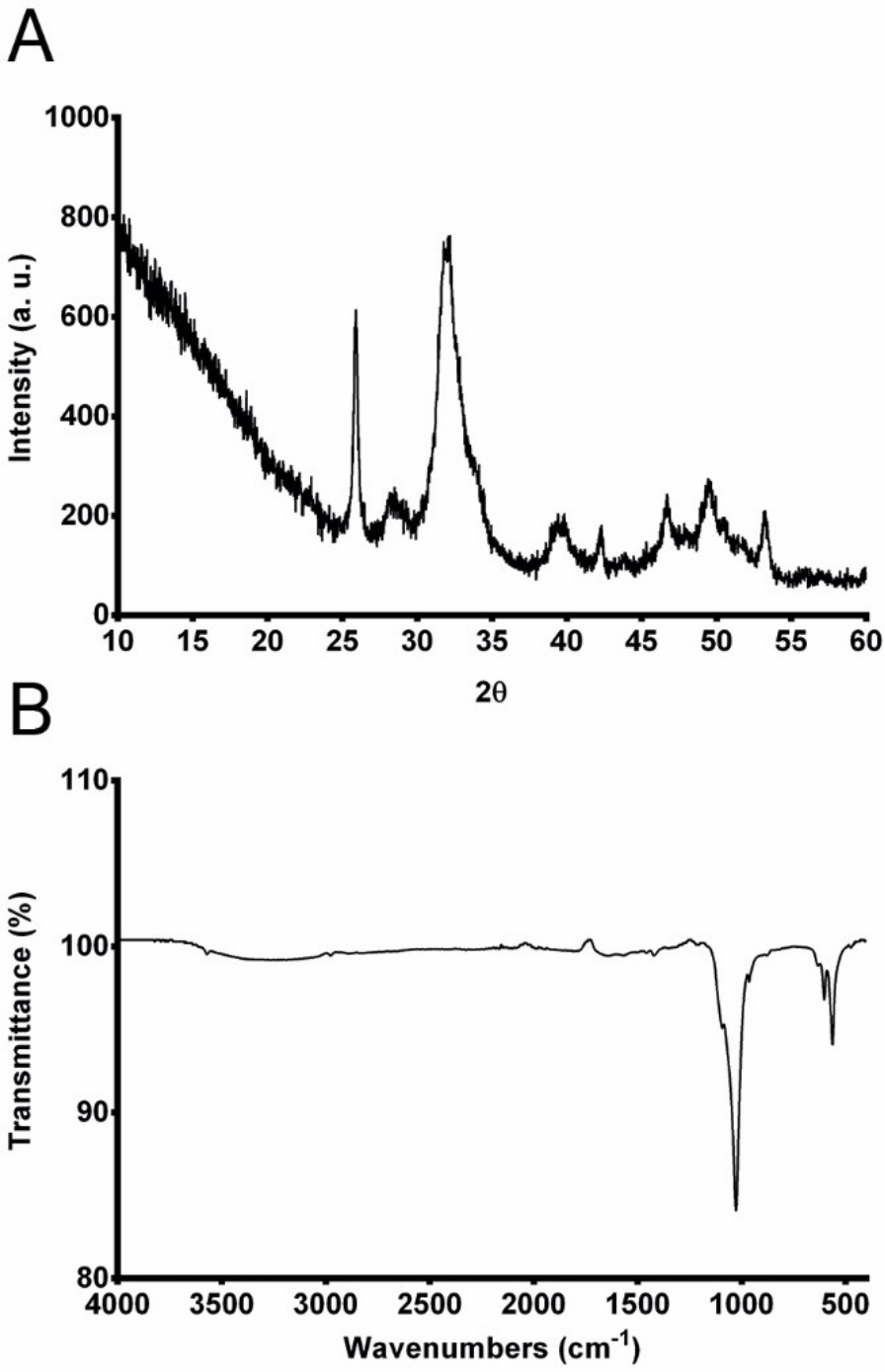

Fig. S1. Characterization of PtPP-loaded HA nanoparticles. A) X-ray diffraction patterns of HA nanoparticles. Main reflection peaks were observed at 26° and 31.9° 2θ corresponding to an apatitic calcium phosphate single phase. B) FT-IR spectra of HA nanoparticles confirmed the presence of the typical absorption bands of apatitic CaP. The spectra showed various phosphate absorption bands at 560-600 cm^{-1}, 962

cm^{-1} and 1000-1100 cm^{-1}, and OH bands at 632 and 3560 cm^{-1} characteristics for hydroxyapatite.

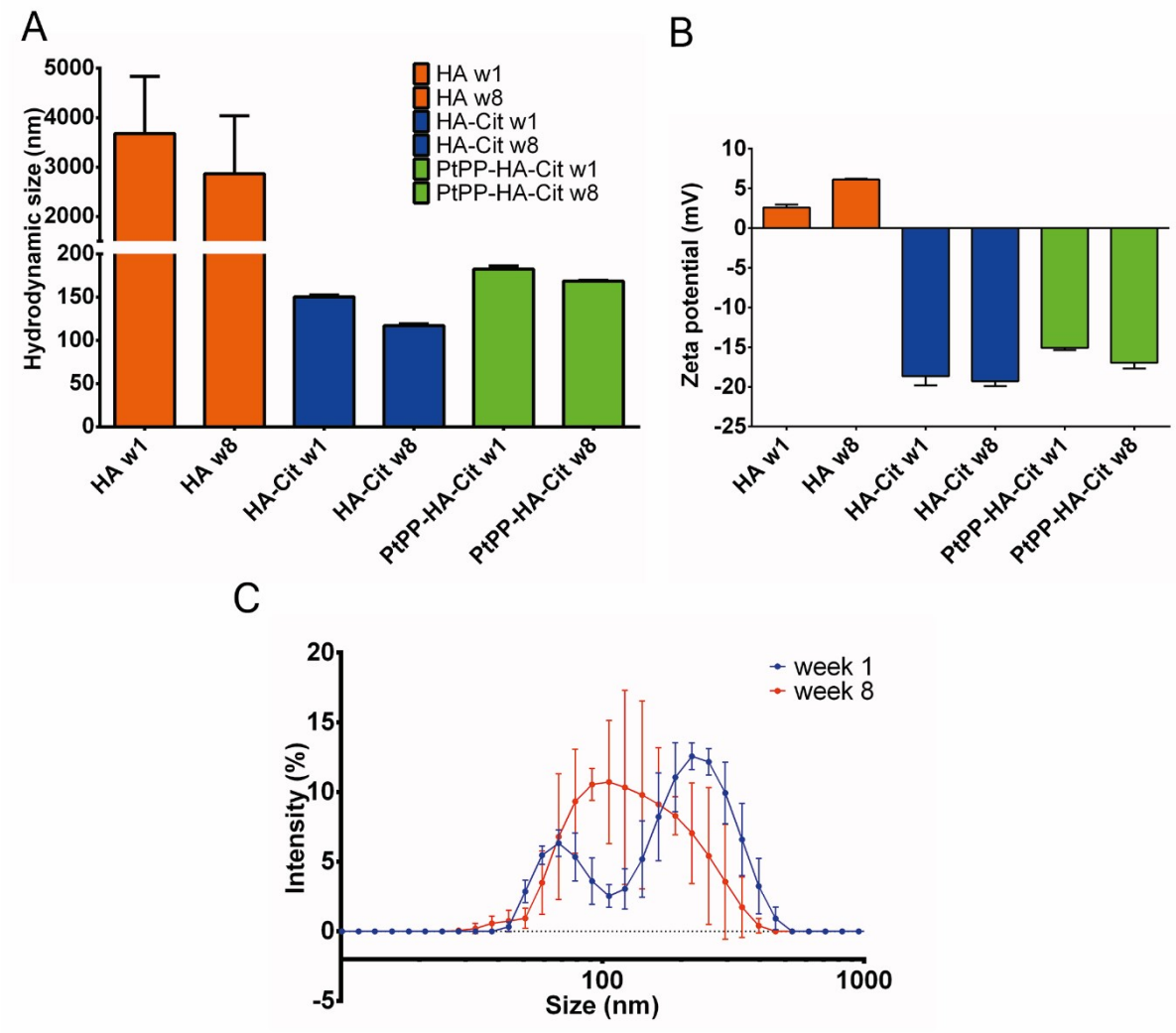

Fig. S2. Stabilization of PtPP-loaded Haps using citrate anions. A) Hydrodynamic size of HA, HA-Cit (after citrate stabilization) and PtPP-HA-Cit (PtPP-loaded on HA-Cit) nanoparticles as measured by means of DLS. Week 1 and week 8 are represented as w1 and w8, respectively. B) Zeta-potential of HA, HA-Cit and PtPP-HA-Cit nanoparticles at 1 mg/ml, 25 °C. C) Size distribution analysis of HA-Cit nanoparticles assessed by DLS. The slight size decrease over time is attributed to slow disaggregation of a population of aggregated nanoparticles. The size distribution analysis performed by DLS evidences that all samples are contain two particle populations, i.e. a major population with a hydrodynamic diameter of ~80nm and a

minor population of aggregated HA nanoparticle clusters with hydrodynamic diameter of ~300nm. Over time the nanoparticles disaggregate, leading to a hydrodynamic size close to the size of single nanoparticles.

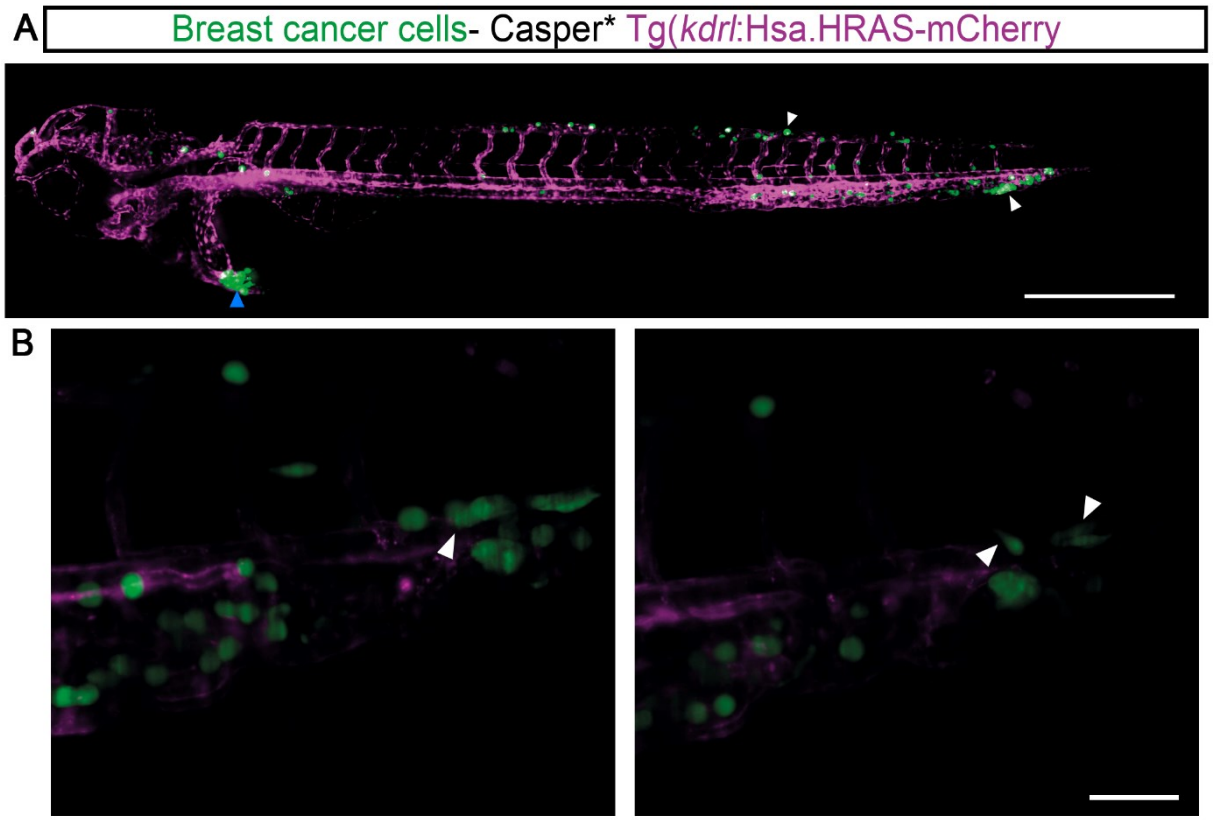

Fig. S3. Breast cancer cells in xenografted zebrafish embryos. A) Representative image of zebrafish embryos expressing vascular marker *Tg*(*kdrl:Has.HRAS-mCherry)* in *casper* background hosting eGFP labeled breast cancer cells (MDA-MB-231_eGFP) at 24 h post injection. Cancer cells injected at the Duct of Cuvier (blue arrowhead) migrated throughout the embryo (white arrowhead). Vasculature is indicated in magenta and breast cancer cells are depicted in green. Scale bar: 500 µm. B) Representative image of breast cancer cells in the caudal tail region (left, white arrowhead) of the embryo exhibiting extravasation by forming protrusion (right, white arrowhead). Scale bar: 50 µm.

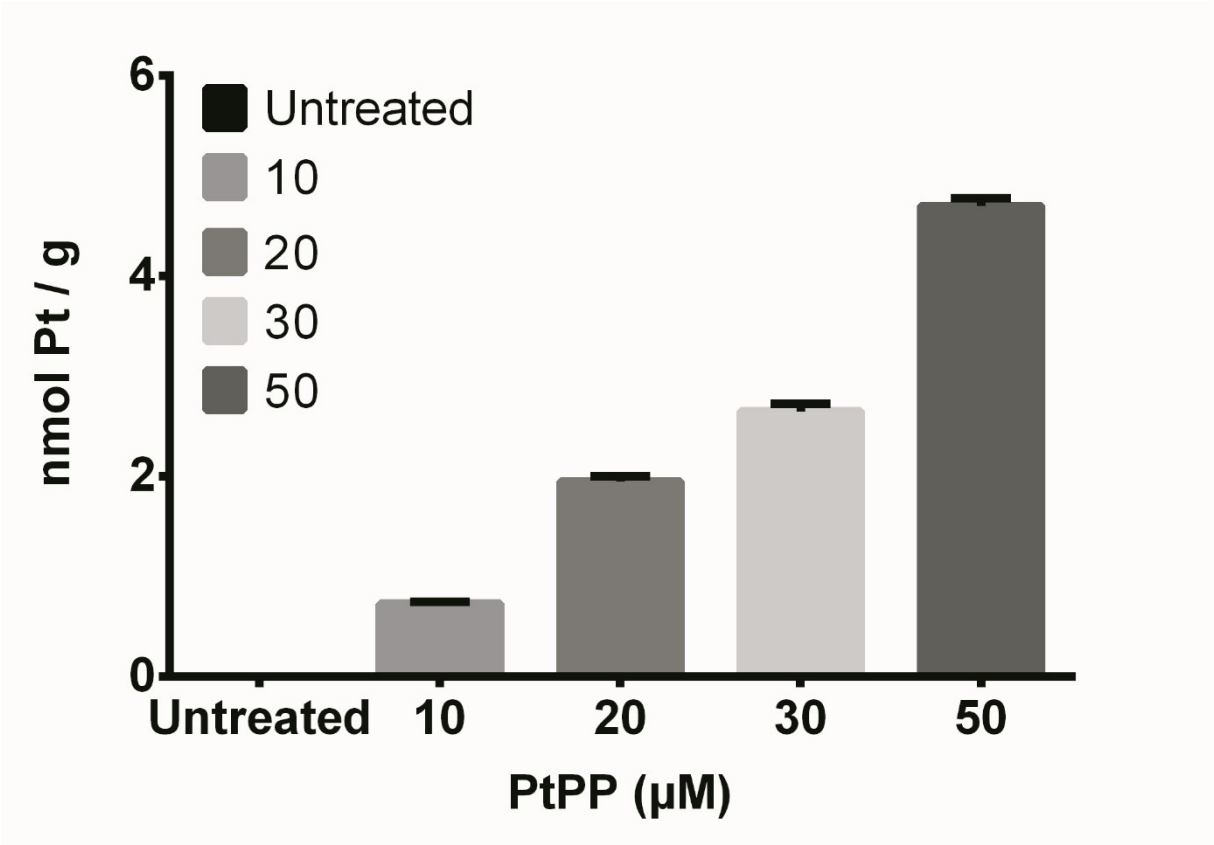

Fig. S4. ICP-MS analysis of PtPP-treated zebrafish embryos. ICP-MS was used to assess platinum amount (expressed at nmol Pt per gram of zebrafish) in the PtPP-treated embryos compared to untreated embryos as control groups. PtPP uptake by zebrafish increased with increasing PtPP concentration.

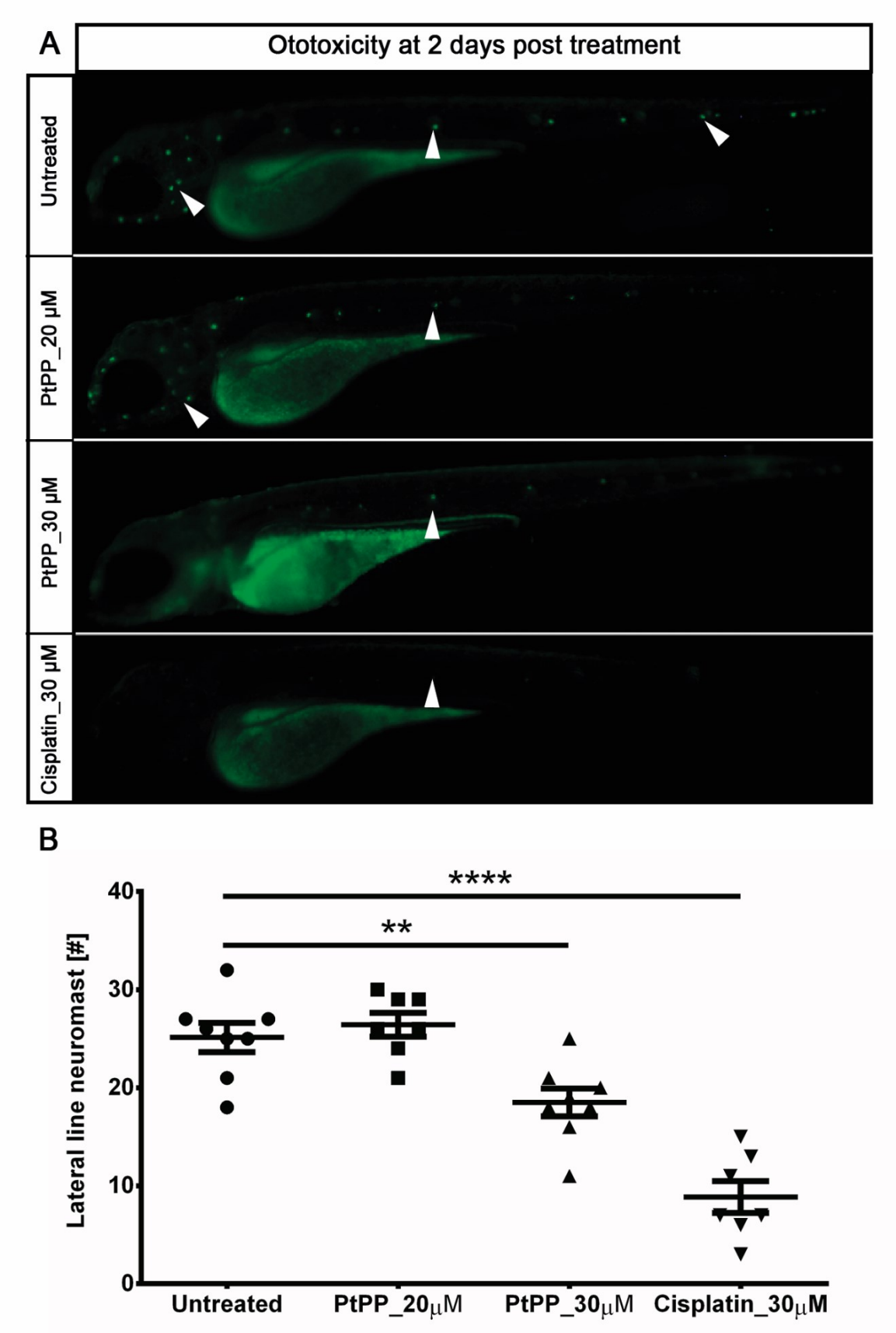
A
Ototoxicity at 2 days post treatment
Untreated
PtPP_20 µM
PtPP_30 µM
Cisplatin_30 µM
B
****
**
Lateral line neuromast [#]
40
30
20
10
0
Untreated
PtPP_20µM
PtPP_30µM
Cisplatin_30µM

Fig. S5. Ototoxicity assay in zebrafish embryos. A) Embryos were treated with PtPP (20 μM and 30 μM) and Cisplatin (positive control, 30 μM) and lateral line neuromasts were stained using DASPEI. Live imaging of these treated, stained embryos showed ototoxic effect of PtPP on the neuromast cells as expressed by a reduced amount of these cells caused by 30 μM of PtPP and cisplatin treatments after 2 days post treatment (neuromast cells indicated with white arrowheads). B) Quantification of the lateral line neuromast cells stained by DASPEI after 2 days post treatment with PtPP and cisplatin. Treatment using 30 μM cisplatin and 30 μM PtPP caused a significant reduction of neuromast cells. The plot represents means ± sem. **0.001 <P < 0.01; ****P <0.0001.

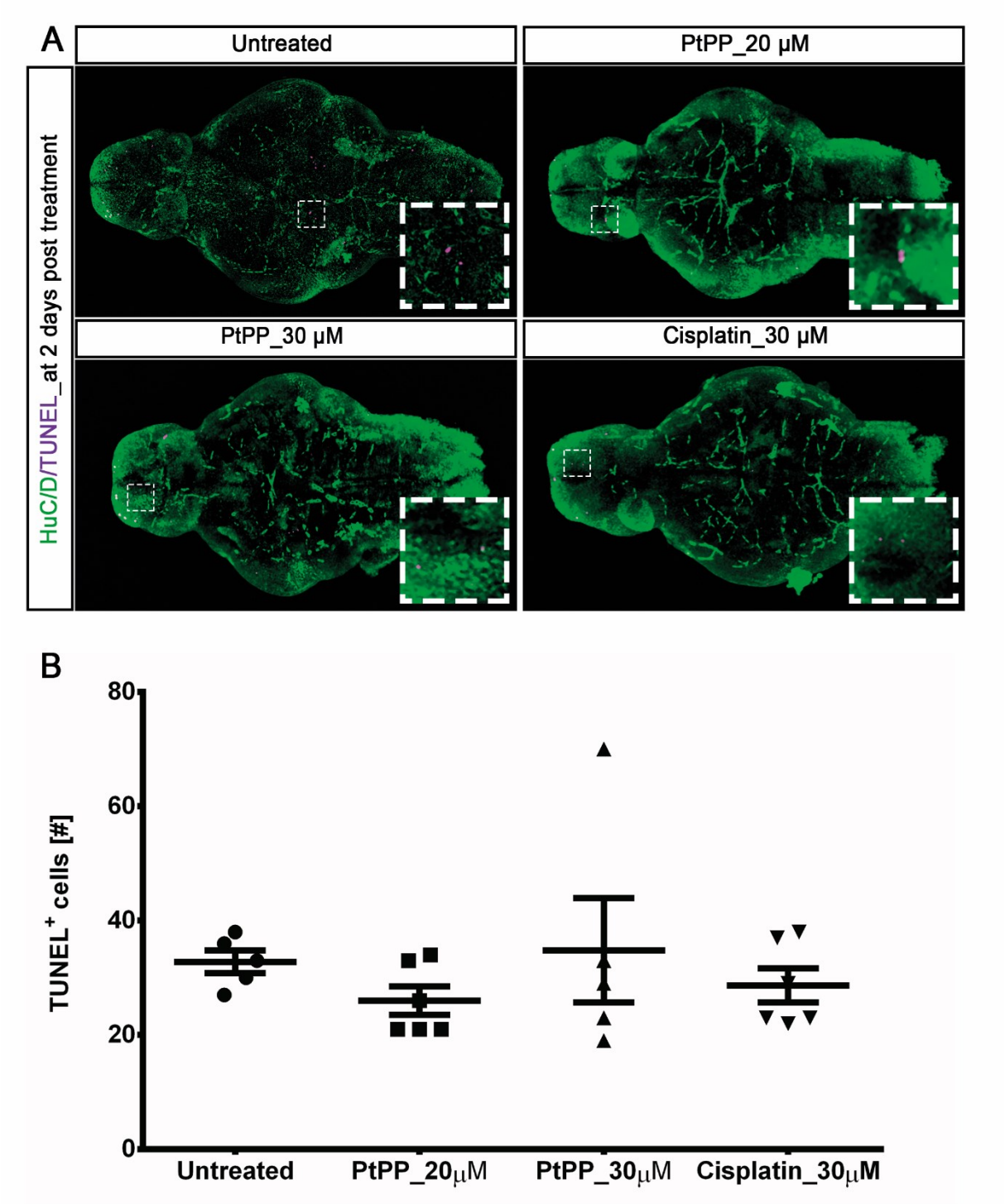

Fig. S6. Cell death in zebrafish larvae brains due to PtPP treatment. A) After PtPP and cisplatin treatments, larvae brains were cleared and stained for apoptotic cells using the TUNEL assay. Confocal imaging of these stained larvae brains showed a basal level of apoptotic cells irrespective of PtPP and cisplatin treatments (indicated by white dashed line boxes pointing at TUNEL+ cells in the brain). Neurons are stained with

HuC/D (green) and apoptotic cells are stained with TUNEL (magenta). Inserts show images at higher magnifications of the areas indicated with a white dashed line box. B) Quantification of the TUNEL+ cells in the zebrafish larvae brain after 2 days post treatment with PtPP and cisplatin. Cisplatin and PtPP treatments did not show any neurotoxic effect.

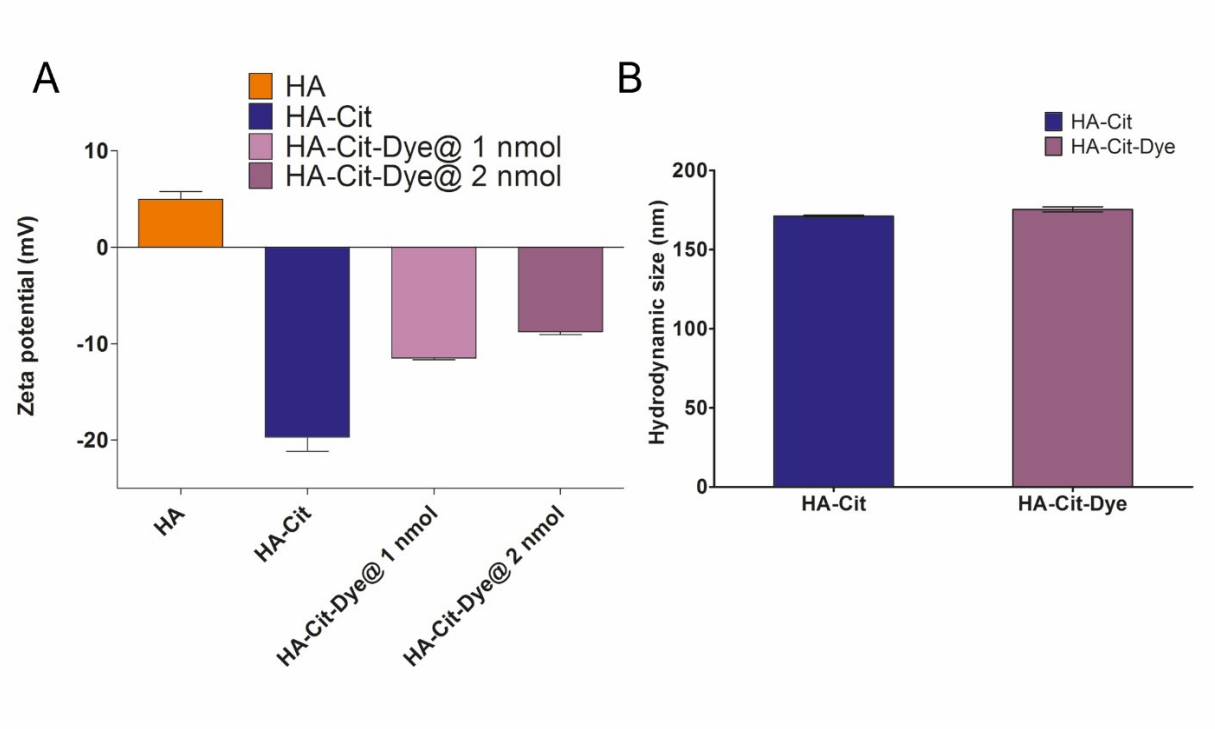

Fig. S7. Fluorescent labeling of HA-Cit and HA nanoparticles. A) Zeta potential of HA, HA-Cit (after citrate stabilization) and HA-Cit-dye (AF647-zoledronate dye-loaded on HA-Cit) at 1 mg/ml, 25 °C. B) Hydrodynamic size of HA-Cit and HA-Cit-Dye as measured by DLS. Labeling of 10 mg of nanoparticles with 1 or 2 nmol of dye resulted into 99% labeling efficiency. The size (171-175 nm) and dispersion (PDI values 0.34-0.35) of the nanoparticles were unaffected by the labeling method, whereas the positively charged fluorescent dye reduced the negative charge of the HA-Cit nanoparticles from -19.3 mV to -11.5 mV and -8.7 mV for 1 and 2 nmol of AF647-zolendronate, respectively. HA-Cit nanoparticles labeled with 1 nmol dye were selected for further studies on the biodistribution of nanoparticles in zebrafish embryos from day 2 to day 4 post fertilization.

Table S1. Size and Zeta potential of HA nanoparticles.

Sample	Size (nm)	PDI	Zeta potential (mV)
HA w1	3682 ± 1154	0.43 ± 0.13	2.43 ± 0.15
HA w8	2865 ± 1174	0.51 ± 0.44	6.11 ± 0.11
HA-Cit w1	150 ± 2	0.3 ± 0.03	-18.57 ± 0.9
HA-Cit w8	117 ± 2	0.21 ± 0.03	-19.30 ± 0.6
HA-Cit-PtPP w1	183 ± 4	0.39 ± 0.01	-15.10 ± 0.26
HA-Cit-PtPP w8	169 ± 1	0.27 ± 0.02	-16.97 ± 0.71

Table S2. Effect of citrate functionalization on drug loading efficiency and colloidal stability of HA nanoparticles using different adsorption strategies.

	Adsorption with PtPP and citrate			**Controls**		
Method/Sample	DF[1]	CF[2]	S[3]	HA only	HA-Cit	HA-PtPP
Ca (wt%)	26.2 ± 0.6	25.4 ± 0.4	30.3 ± 1	32.1 ± 0.5	31.6 ± 1.5	32.4 ± 0.9
P[4] (wt%)	11.9 ± 0.1	12.9 ± 0.8	12.9 ± 0.4	14.9 ± 0.2	14.1 ± 0.4	16.8 ± 0.5
Pt (wt%)	2.4 ± 0.1	3.5 ± 0.2	0.9 ± 0.1	-	-	3.7 ± 0.1
Ca/P ratio	1.7 ± 0.1	1.5 ± 0.1	1.8 ± 0.2	1.7 ± 0.1	1.7 ± 0.1	1.5 ± 0.1
Drug loading efficiency (wt%)	8.9 ± 0.7	8.2 ± 0.6	2.7 ± 0.1	-	-	11.3 ± 0.3
Size (nm)	183 ± 3.5	1260 ± 80	400 ± 30	5600 ± 1000	470 ± 30	4800 ± 490
Polydispersity Index	0.4 ± 0.1	0.7 ± 0.1	0.5 ± 0.1	0.4 ± 0.2	0.8 ± 0.2	0.4 ± 0.2
Zeta potential (mV)	-15.1 ± 0.3	-12.4 ± 0.2	-23.2 ± 0.2	-0.1 ± 0.2	-17.5 ± 0.4	-4.2 ± 0.3

[1]Drug first

[2]Citrate first

[3]Simultaneous adsorption

[4]P content is influenced by pyrophosphate ligand of PtPP

Table S3. Cumulative release (%) of Platinum (Pt) and Calcium (Ca) from PtPP-loaded HA nanoparticles at pH 6.5 and 7.4.

Time (h)	% Ca, pH 6.5	% Ca, pH 7.4	% Pt, pH 6.5	% Pt, pH 7.4
0	0.00 ± 0.0	0.00 ± 0.0	0.00 ± 0.0	0.00 ± 0.0
24	7.34 ± 0.1	1.84 ± 0.2	30.39 ± 0.2	33.71 ± 0.4
72	9.45 ± 0.1	2.25 ± 0.3	70.04 ± 0.1	66.45 ± 0.7
168	25.50 ± 0.3	3.63 ± 0.4	77.94 ± 0.3	70.72 ± 0.6

Table S4. Viability and proliferation of breast cancer cells treated with Pt-free HA nanoparticles.

pH	**Viability (%)**		**Proliferation (%)**	
	24 h	**72 h**	**24 h**	**72 h**
7.4	95.9 ± 8.0	101.9 ± 8.0	95.2 ± 9.9	99.4 ± 4.9
6.5	96.1 ± 3.8	98.9 ± 5.8	88.4 ± 6.0	94.5 ± 3.7

Table S5. Viability and proliferation of breast cancer cells with no treatment.

pH	**Viability (%)**		**Proliferation (%)**	
	24 h	**72 h**	**24 h**	**72 h**
7.4	96.6 ± 5.4	91.8 ± 3.8	100 ± 11.8	100 ± 4.6
6.5	100 ± 3.4	100 ± 4.2	100 ± 8.6	100 ± 9.1

References:

1. J. A. Harris, A. G. Cheng, L. L. Cunningham, G. MacDonald, D. W. Raible and E. W. Rubel, *J Assoc Res Otolaryngol*, 2003, **4**, 219-234.